Examination of the Change of the Characteristic X-Rays of the Zinc in Fluorine- and Boron-Doped ZnO Thin Films

Ö. Söğüt[a,*], S. Kerli[b], E. Cengiz[c,d] and G. Apaydin[c]

[a]Kahramanmaraş Sutcu Imam University, Faculty of Science and Letters, Department of Physics, 46100 Kahramanmaraş, Turkey

[b]Kahramanmaras Sutcu Imam University, Elbistan Technology Faculty Energy Systems Engineering, 46300 Kahramanmaraş, Turkey

[c]Karadeniz Technical University, Faculty of Science, Department of Physics, 61080 Trabzon, Turkey

[d]Alanya Alaaddin Keykubat Üniversitesi, Faculty of Engineering, Department of Fundamental Sciences, 07450 Antalya, Turkey

(Received August 31, 2016; revised version July 28, 2017; in final form March 5, 2018)

In this study, K_β/K_α X-ray intensity ratios of zinc in pure zinc, undoped ZnO thin film and boron and fluorine-doped ZnO thin films have been investigated. These samples have been excited by 59.5 keV γ-rays from a ^{241}Am annular radioactive source. K X-rays emitted by the samples have been counted using an Ultra-LEGe detector with a resolution of 150 eV at 5.9 keV. The K_β/K_α X-ray intensity ratios of the doped ZnO thin films have been compared with that of the undoped ZnO thin film. The deviations between the results can be explained by delocalization and/or charge transfer phenomena causing change in valence electronic configuration of zinc.

DOI: 10.12693/APhysPolA.133.1124

PACS/topics: 32.30.Rj, 78.70.En, 32.30.–r, 32.80.Fb

1. Introduction

Recently, thin film science has grown worldwide into a major research area. The importance of the coatings and the synthesis of new materials for industry have resulted in a tremendous increase of innovative thin film processing technologies [1–3]. ZnO is an n-type wide band gap semiconductor with a wide direct band gap of 3.37 eV at room temperature and large exciton binding energy of 60 meV [4]. ZnO thin films are materials widely used in numerous applications such as piezoelectric transducers, optical waveguides acousto-optic media, surface acoustic wave devices, conductive gas sensors, transparent conductive electrodes, solar cell windows, and varistors [5–9]. Many researchers have added dopant such as Li, B, N, F, P, Mg, Co, Cu, Ge, In, Te, and Zr to the ZnO thin films for improving or changing the film's hardness, conductivity and optical, electronic, and electrical properties [5, 8, 10–13].

Energy dispersive X-ray fluorescence (EDXRF) method and K shell fluorescence parameters such as X-ray intensity ratios, fluorescence yields, cross-sections, and vacancy transitions can be used to provide useful information on the electronic structure of Zn transition metal in the doped and undoped ZnO thin films. It is well known that the X-ray fluorescence parameters depend on the physical and chemical environments of the elements in a sample. This dependence can be explained as due to changes of the 3d-electron population in the transition metal.

When looked at the literature, there are a lot of investigations on the characteristic X-ray parameters of the thin film alloys or thin films. The K_β/K_α intensity ratios of Ti, Cr and Ni in Cr_xNi_{1-x} and Ti_xNi_{1-x} were measured by Bhuinya and Padhi [14]. They explained the results according to the charge transfer. Söğüt et al. [15] investigated the alloying effects on K_β/K_α intensity ratios in Cr_xNi_{1-x} and Cr_xAl_{1-x} alloys and they reported that K X-ray intensity ratios vary depending on the concentrations of elements in the alloys. Raj et al. [16] determined the valence electronic structure of Fe and Ni in Fe_xNi_{1-x} using relative K X-ray intensity ratios. They observed changes in 3d-electron population of Fe and Ni for certain alloy compositions. Pawlowski et al. [17] determined the K_β/K_α intensity ratios of Ti, Cr, Fe and Co in some alloys. They report that the observed changes in the valence structure are due to the rearrangement of electrons between 3d and (4s, 4p) states of individual metal atoms. Furthermore, the investigations from K to L shell/subshells vacancy transitions of Zn and Fe in Fe_xZn_{1-x} thin film alloys were done by Söğüt [18]. Dogan et al. [19] measured the K shell production cross-sections and K_β/K_α intensity ratios of Cr and Zn in different alloy compositions. They also calculated empirical and semi-empirical K-shell fluorescence yields and K_β/K_α intensity ratios. Cengiz et al. [20] investigated the K shell fluorescence parameters of porous Ni–49 at.% Ti shape memory alloys using EDXRF technique. The structure analyses of the alloys were made

*corresponding author; e-mail: omersogut@gmail.com

using X-ray diffraction (XRD) and X-ray photoelectron spectroscopy (XPS). They attributed the deviations between the experimental results and theoretical values of pure Ti and Ni to charge transfer phenomena and/or rearrangement of valence shell electrons and porosity.

The aim of this study is to investigate the variation of K_β/K_α X-ray intensity ratios of zinc in boron and fluorine doped ZnO thin films by using XRF technique according to the doping amount of boron and fluorine. The obtained values were compared with the value of undoped ZnO thin film.

2. Experimental details

2.1. Sample preparation

ZnO thin films were fabricated on glass substrates by using the airbrush spraying. The deposition of films was carried out in ambient air and under a fume hood. The base ZnO solution was prepared by dissolving 0.1 M zinc chloride ($ZnCl_2$) in distilled water. For doping, 0.1 M of boric acid (H_3BO_3) and a 0.1 M of ammonium fluoride (NH_4F) are dissolved in distilled water and they were added to the base solution in appropriate atomic ratio. The atomic ratios of F/(Zn + B) in the solution are adjusted by changing F (1, 2, 3, 4, and 5 at.%) and B (2, 3, 4, and 5 at.%) concentrations. The starting solution was sprayed onto heated substrates at 450 °C by using an airbrush spray with pressurized air. To keep the substrate temperature constant, the precursor solution was deposited cyclically, 8 s of spraying followed by 50 s without spraying. The spray nozzle to substrate distance was adjusted to 35 cm, and to get the uniform film in thickness the lateral speed of the airbrush was set to 1 cm/s and the volumetric spray rate was set to approximately 0.3 ml/s by adjusting the air pressure. It has been shown that the thin films are in hexagonal wurtzite structure and are in accordance with the reference given in the PDF-2:01-079-2205 in previous work of Kerli et al. [4]. The spraying process was repeated 20 times to get the film about 1 μm thickness (Fig. 1).

2.2. XRF measurements

The boron and fluorine-doped ZnO thin film samples were irradiated by 59.5 keV photons emitted by 50 mCi ^{241}Am radioactive source. The characteristic X-rays emitted from the target were detected using an Ultra-LEGe detector (active area is 30 mm^2, thickness is 5 mm, and polymer window thickness is 0.4 μ m). The measured energy resolution of the detector system is 150 eV at full-width half maximum for the Mn K_α line at 5.9 keV. The output from the preamplifier, with pulse pileup rejection capability, was fed to a multichannel analyzer interfaced with a computer provided with software for data acquisition and peak analysis. The sample was placed at 45° angles with respect to the direct beam and fluorescent X-rays emitted 90° to the detector. All the samples were measured at least three times and in order to minimize the statistical errors, the averages of measurements were taken [3]. K X-ray spectra of zinc in ZnO thin film doped with 4% fluorine are shown in Fig. 2. The K_β/K_α X-ray intensity ratios have been calculated by using the following equation:

$$\frac{I(K_\beta)}{I(K_\alpha)} = \frac{N(K_\beta)}{N(K_\alpha)}\frac{\varepsilon(K_\beta)}{\varepsilon(K_\alpha)}\frac{\beta(K_\beta)}{\beta(K_\alpha)}, \quad (1)$$

where $N(K_\alpha)$ and $N(K_\beta)$ are counts observed under the peaks corresponding to K_α and K_β X-rays, respectively, and $I_0G_\varepsilon K_\alpha$ and $I_0G_\varepsilon K_\beta$ are the efficiencies of the detector for the K_α and K_β series of X-rays, respectively (since I_0G is a constant value for during the experiment, it is not written in Eq. (1) because it is abbreviated in Eq. (1)). I_0 is the intensity of the incident radiation and G is a geometrical factor. $\beta(K_\alpha)$ and $\beta(K_\beta)$ are the target self-absorption correction factors for both the incident and the emitted radiations. The target self-absorption correction factors and the efficiencies of the detector have been calculated as in the previous paper [18]. K X-ray spectra of Zn in ZnO thin film doped 4% fluorine are given in Fig. 2.

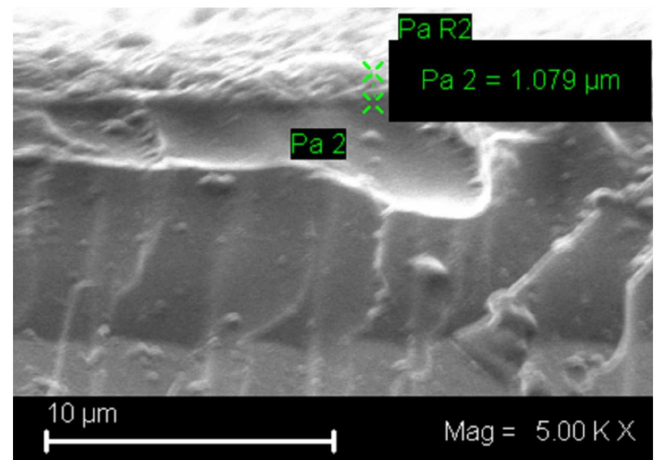

Fig. 1. Cross-section SEM image of a thin film.

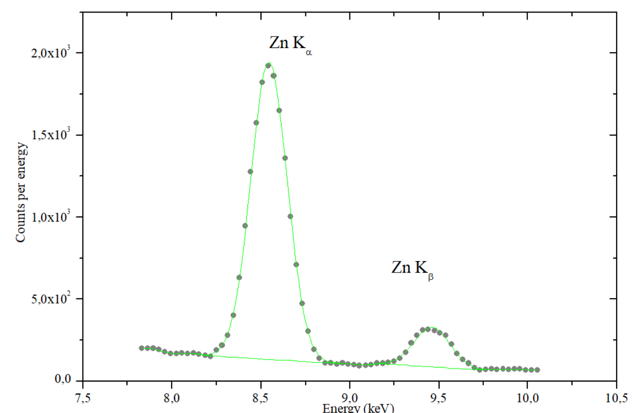

Fig. 2. K X-ray spectra of zinc in ZnO thin film doped 4% fluorine.

3. Results and discussion

In this study, the K_β/K_α X-ray intensity ratios of zinc in pure Zn, ZnO thin film and fluorine- and boron-doped ZnO thin films have been determined. The present results are given for pure Zn and ZnO thin film, and the fluorine- and boron-doped ZnO thin films in Table I and Table II, respectively. Possible sources of error in the determined the K_β/K_α X-ray intensity ratio are IG_ε determination (<1–2%), background determination (<1%), self-absorption (<1–2%), and counting statistics (<1%). The total experimental relative error is estimated to be 4–6%.

TABLE I

K_β/K_α X-ray intensity ratios of pure Zn and ZnO thin film.

K_β/K_α X-ray intensity ratios							
Sample	Present paper	Theor.	Experimental				
		Scofield [21]	Ertuğrul et al. [24]	Khan et al. [22]	Söğüt et al. [25]	Rebohle et al. [23]	Porikli et al. [26]
Zn	0.1338±0.0096	0.1241	0.1360	0.1320	0.1254	0.1528	0.1359
ZnO	0.1148±0.0068	-	-	-	-	0.1487	-

It is shown from Table I that the experimental values of the K_β/K_α X-ray intensity ratios for pure zinc agree with the theoretical value of Scofield and the other experimental values for pure zinc. On the other hand, the experimental K_β/K_α X-ray intensity ratio value of the undoped ZnO thin film is much lower than that of the pure zinc. This can be due to influence of oxidation [23]. The present situation is also shown between the K_β/K_α X-ray intensity ratios of the undoped ZnO thin film and the theoretical value of Scofield. The reason is that Scofield has calculated the intensity ratios for pure Zn elements; so, it does not show the dependence on the formal oxidation number. Besides, the deviations between the present and other experimental values can arise from a different detector type, a different exciting energy, a different detector efficiency and precision in measurements as well as the sample difference.

The experimental K_β/K_α X-ray intensity ratios of Zn in fluorine- and boron-doped ZnO thin films and relative K_β/K_α X-ray intensity ratios with respect to undoped ZnO thin film are given in Table II. The results show that there is a lack of consistency between undoped ZnO thin film and doped ZnO thin films. For fluorine concentrations from 1% to 3% the K_β/K_α X-ray intensity ratios of Zn is lower than that of undoped ZnO thin film, whereas for other two fluorine concentrations the values are higher. However, when the amounts of fluorine doping increase, the intensity ratios increase as shown in Fig. 3. The K_β/K_α X-ray intensity ratios of Zn for 2% boron-doped ZnO thin film is higher than that of undoped ZnO thin film. For boron doping from 3% to 5 % the values of the intensity ratios are lower. On the other hand, as the amounts of boron doping increases from 2% to 5%, the values of intensity ratios decrease as shown in Fig. 3. When boron-doped is 1% and fluorine-doped are changed by 1% to 3%, the K_β to K_α X-ray intensity ratios of Zn in ZnO:B:F are lower than that of undoped ZnO thin film. If boron-doped is 2% and fluorine-doped are changed from 1% to 3%, the K_β to K_α X-ray intensity ratio of Zn for 1% fluorine doping is higher than that of undoped ZnO thin film, for others they are lower.

TABLE II

K_β/K_α X-ray intensity ratios of fluorine- and boron-doped ZnO thin film ($(I_{K_\beta}/I_{K_\alpha})_A$ experimental K_β-to-K_α X-ray intensity ratios and $(I_{K_\beta}/I_{K_\alpha})_B$ relative K_β-to-K_α X-ray intensity ratios with respect to ZnO thin film)

K_β/K_α X-ray intensity ratios				
Sample	Amount of doping F [%]	Amount of doping B [%]	$(I_{K_\beta}/I_{K_\alpha})_A$	$(I_{K_\beta}/I_{K_\alpha})_B$
ZnO	-	-	0.1148±0.0068	1.0000
ZnO:F	1	-	0.1057±0.0079	0.9207
ZnO:F	2	-	0.1084±0.0048	0.9443
ZnO:F	3	-	0.1128±0.0090	0.9826
ZnO:F	4	-	0.1178±0.0106	1.0261
ZnO:F	5	-	0.1195±0.0117	1.0409
ZnO:B	-	2	0.1171±0.0104	1.0200
ZnO:B	-	3	0.1072±0.0084	0.9337
ZnO:B	-	4	0.1043±0.0073	0.9085
ZnO:B	-	5	0.1010±0.0098	0.8798
ZnO:B:F	1	1	0.1114±0.0108	0.9704
ZnO:B:F	2	1	0.1106±0.0087	0.9634
ZnO:B:F	3	1	0.1091±0.0071	0.9503
ZnO:B:F	1	2	0.1211±0.0920	1.0549
ZnO:B:F	2	2	0.1144±0.0093	0.9965
ZnO:B:F	3	2	0.1110±0.0101	0.9669

Besides, as the amounts of fluorine doping increase and the amounts of boron doping are constant, the intensity ratio values decrease as shown from Fig. 4. The inconsistency between the intensity ratios of undoped ZnO thin film and doped ZnO thin films can be explained by changing in $3d$ electron population due to delocalization and/or charge transfer [16]. The crystal structure of the undoped ZnO thin film has wurtzite hexagonal. Boron and fluorine doping did not change the structure. However, as seen from Table I, the intensity ratios of ZnO thin films has increased and decreased by the concentrations of F and B doping, respectively. This indicates that the fluorine and

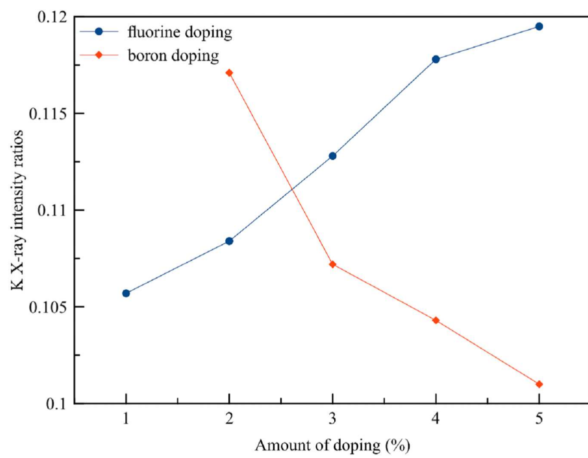

Fig. 3. The change of K_β/K_α X-ray intensity ratios of Zn according to the amounts of fluorine and boron doping in ZnO thin films.

boron which enter the structure and replace with oxygen has changed the crystal parameters [4]. Fluorine has a bigger electronegativity value than oxygen, so it attracts more valence electrons than oxygen. Boron has a smaller electronegativity value than oxygen and a smaller from that of zinc, so it attracts less electron than oxygen. This causes the valence electronic structure of zinc to change, thus resulting in changes in the K_β/K_α X-ray intensity ratios of Zn in fluorine- and boron-doped ZnO thin films.

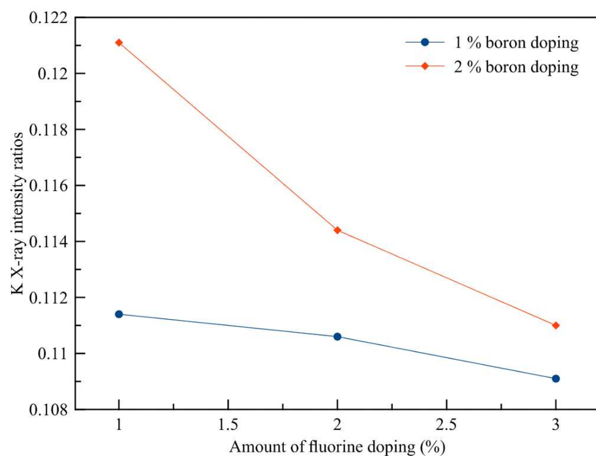

Fig. 4. The change of K_β/K_α X-ray intensity ratios of Zn according to the amounts of fluoride doping in ZnO thin films (amount of boron doping was fixed at 1 and 2%).

4. Conclusion

In this study, the K_β/K_α X-ray intensity ratios of zinc in pure Zn, undoped ZnO thin film and fluorine- and boron-doped ZnO thin films have been determined. The experimental values of the intensity ratios of pure zinc agree with the theoretical value and the other experimental values. The lack of consistency between the experimental values of pure zinc and the undoped ZnO thin film can arise from the influence of oxidation. Besides, the reason in the deviations between the intensity ratios of the undoped and doped thin films can be from change in the valence electronic configuration due to delocalization and/or charge transfer.

Acknowledgments

This work was supported by Scientific Research Fund of Kahramanmaras Sutcu Imam University, Turkey (project No. 2012/4-3 YLS), and all the authors are thankful for this support.

References

[1] T. Wagner, *Thin Film Science* Max-Planck Institut für Metallforschung, Stuttgart 1999.

[2] I.H. Karahan, K. Karabulut, *U. Alver, Phys. Scr.* **79**, 055801 (2009).

[3] Ö. Söğüt, C. Donuk, G. Apaydın, O.F. Bakkaloğlu, *Can. J. Phys.* **92**, 435 (2014).

[4] S. Kerli, U. Alver, A. Tanrıverdi, B. Avar, *Protect. Met. Phys. Chem. Surf.* **50**, 797 (2014).

[5] S. Zhao, Y. Zhou, Y. Liu, K. Zhao, S. Wang, W. Xiang, Z. Liu, P. Han, Z. Zhang, Z. Chen, H. Lu, K. Jin, B. Cheng, G. Yang, *Appl. Surf. Sci.* **253**, 726 (2006).

[6] S. Mondal, K.P. Kanta, P. Mitra, *J. Phys. Sci.* **12**, 221 (2008).

[7] C.Y. Tsay, K.S. Fan, *Mater. Trans.* **49**, 1900 (2008).

[8] S. Benramache, B. Benhaoua, *Superlatt. Microstruct.* **52**, 807 (2012).

[9] S. Sönmezoğlu, E. Akman, *Appl. Surf. Sci.* **318**, 319 (2014).

[10] J.R. Duclère, M. Novotny, A. Meaney, R. O'Haire, E. McGlynn, M.O. Henry, P.J. Mosnier, *Superlatt. Microstruct.* **38**, 397 (2005).

[11] T. Yamada, T. Nebiki, S. Kishimoto, H. Makino, K. Awai, T. Narusawa, T. Yamamoto, *Superlatt. Microstruct.* **42**, 68 (2007).

[12] S. Abed, M.S. Aida, K. Bouchouit, A. Arbaoui, K. Iliopoulos, B. Sahraoui, *Opt. Mater.* **33**, 968 (2011).

[13] S. Benramache, B. Benhaoua, F. Chabane, *J. Semicond.* **33**, 093001 (2012).

[14] C.R. Bhuinya, H.C. Padhi, *J. Phys. B At. Mol. Opt. Phys.* **25**, 5283 (1992).

[15] Ö. Söğüt, E. Buyukkasap, A. Kucukonder, M. Ertuğrul, Ö. Şimşek, *Appl. Spectrosc. Rev.* **30**, 175 (1995).

[16] S. Raj, H.C. Padhi, M. Polasik, F. Pawlowski, D.K. Basa, *Solid State Commun.* **116**, 563 (2000).

[17] F. Pawlowski, M. Polasik, S. Raj, H.C. Padhi, D.K. Basa, *Nucl. Instrum. Methods Phys. Res. B* **195**, 367 (2002).

[18] Ö. Söğüt, *Radiochim. Acta* **97**, 695 (2009).

[19] M. Dogan, E. Tirasoglu, I.H. Karahan, N.K. Aylıkcı, V. Aylıkcı, A. Kahoul, H.A. Cetinkara, O. Serifoglu, *Radiat. Phys. Chem.* **87**, 6 (2013).

[20] E. Cengiz, O.M. Özkendir, M. Kaya, E. Tirasoglu, I.H. Karahan, S. Kimura, T. Hajiri, *J. Electron. Spectrosc. Relat. Phenom.* **192**, 55 (2014).

[21] J.H. Scofield, *At. Data Nucl. Data Tables* **14**, 94550 (1974).

[22] M.R. Khan, M. Karimi, *X-ray Spectrom.* **9**, 33 (1980).

[23] L. Rebohle, U. Lehnert, G. Zschornack, *X-ray Spectrom.* **25**, 295 (1996).

[24] M. Ertuğrul, Ö. Söğüt, Ö. Şimşek, E. Büyükkasap, *J. Phys. B At. Mol. Opt. Phys.* **34**, 909 (2001).

[25] Ö. Söğüt, E. Büyükkasap, H. Erdoğan, *Radiat. Phys. Chem.* **64**, 343 (2002).

[26] S. Porikli, Y. Kurucu, *Instrument. Sci. Technol.* **36**, 341 (2008).